Comparison of the crystal structure and electronic interband transitions of Ca_2Si thin semiconductor films on $Al_2O_3(0001)$ and Si(111) substrates

N.G. Galkin, K.N. Galkin, O.V. Kropachev, I.M. Chernev, D.L. Goroshko, E.Yu. Subbotin and S.A. Dotsenko

Institute for Automation and Control Processes, 5 Radio St., Vladivostok 690041, Russia

e-mail: galkin@iacp.dvo.ru

Abstract

The method of transforming a ***sacrificial*** **2D Mg_2Si** layer into a ***Ca_2Si template*** was used to form oriented **Ca_2Si** films on *Si(111)* and, for the first time, on ***Al_2O_3(0001)*** with the preliminary formation of an amorphous **2D Si layer**. It has been found that a ***Ca_2Si template*** on both types of substrates makes it possible to grow ***oriented Ca_2Si*** films (**45-170 nm**) by molecular beam epitaxy. The effect of the ratio of ***Ca*** to ***Si*** ***deposition rates*** on the ***single-phase Ca_2Si films*** on the *Si(111)* substrate at **250 °C** was shown. An upper limit has been established for such a ratio (**4.0**), at which **Ca_2Si(100)** film is epitaxially formed. Studies of the *optical properties* and the ***Ca_2Si*** *energy band structure* parameters on **sapphire** reviled the nature of the fundamental direct transition with an energy of **0.88 eV**. It has been established that ***four direct interband transitions*** are observed in the ***Ca_2Si*** band structure: **0.88**, **1.16**, **1.49** and **1.61 eV**. The results obtained are essential to fabricate ***Ca_2Si/Si*** heterostructures for *optoelectronics* and nanophotonics in the ***near-IR region*** of the spectrum.

Introduction

Calcium silicides form six compounds **Ca_2Si**, **CaSi**, **Ca_5Si_3**, **Ca_3Si_4**, **$Ca_{14}Si_{19}$** and **$CaSi_2$** [1]) with different crystal structure and composition and have a wide range of properties from semiconductor [**2**] to semimetallic [**3**]. Semiconductor silicides with different band gaps include (Ca_2Si, Ca_3Si_4, Ca_5Si_3 and $Ca_{14}Si_{19}$) [**2,3**], among which Ca_2Si is currently attracting the main attention [**4**]. According to ab initio theoretical calculations, Ca_2Si is a direct-gap semiconductor with a band gap from 0.30 - 0.36 eV [**5**] to 1.02 eV [**6**].

[1] P. Manfrietti, M.L. Fornasini, A. Palenzona, Intermetallics **8**(2000)223.

[2] S. Lebegue, Phys. Rev. B. **72**(2005)085103.

[3] O. Bisi, L. Braikovich, et.al. Phys. Rev. B. **40**(1989)10194.

[4] C. Wen, T. Nonomura, et.al. Physics Procedia **11**(2011)106.

[5] D.B. Migas, et.al. Jpn. J. Appl. Phys. **54**(2015)07JA03.

[6] S. Lebegue, et.al. Phys. Rev. B **72**(2005)085103.

However, the direct band structure has not yet been confirmed by experimental data. Semiconductor epitaxial **Ca_2Si** films on a ***Si(111)*** substrate have recently been grown through the formation of a two-dimensional sacrificial **Mg_2Si** layer [**7,8**] and its transformation into **Ca_2Si**, followed by growth to thick **Ca_2Si** films by molecular beam epitaxy at **250°C** [**8**]. For grown thick epitaxial **Ca_2Si** films, the ***first direct interband transition*** was determined at energy of **1.095 eV**, which, however, **is not fundamental** due to the ***high density of defect states at 0.5–1.0 eV***. To establish the nature of the fundamental interband transition in **Ca_2Si** films at photon energies ***below 1.0 eV***, it is necessary to grow them on a ***transparent substrate***, for example, **sapphire** (***Al_2O_3(0001)***).

[7] S.A. Dotsenko, et.al. Physics Procedia 11(2011)95.
[8] N.G. Galkin, K.N. Galkin, S.A. Dotsenko, et.al. Mat. Sci. Sem. Proc., 113(2020)105036.

1. Experimental

The growth of Ca_2Si films was carried out in an ultrahigh vacuum (UHV) chamber of an OMICRON Compact setup with a base vacuum of 2×10^{-11} Torr, equipped with a LEED and AES/EELS analyzer, a block of molecular beam sources of silicon (Si), magnesium (**Mg**), and calcium (**Ca**) by carrying out the deposition of Mg, Ca and Si on a single-crystal sapphire - ***Al_2O_3(0001)*** or a ***Si(111)*** substrate in various temperature conditions.

In all growth experiments, Knudsen cells were used as evaporative sources of **Mg** and **Ca** with direct current passing through a resistive heating element. The deposition rates of **Mg**, **Ca**, and **Si**, calibrated with quartz thickness sensors, were (**0.4–0.75**) nm/min, (**0.1–8.4**) nm/min, and (**0.4–0.9**) nm/min, respectively, in different experiments.

Ca_2Si films on silicon substrates with the (111) orientation were grown using the method of transformation of a ***sacrificial 2D Mg_2Si layer*** into a ***Ca_2Si template*** followed by co-deposition of **Ca** and **Si** atoms, which was tested in [9]. This technique was modified for the growth of **Ca_2Si** on sapphire. A thin layer of amorphous silicon 10 nm thick was deposited first on an atomically-clean sapphire surface at room temperature, on which a small flow of **Mg** was deposited by reactive epitaxy at **150°C** to form a ***Mg_2Si layer***. The reactive deposition of **Ca** atoms at a low rate and **T= 250°C** was sufficient to convert the ***sacrificial 2D Mg_2Si layer*** on sapphire into a ***Ca_2Si template*** with the following growth of a thicker **Ca_2Si** film by the ***MBE*** method.

2. Results and Discussion

2.1 Morphology, structure and optical properties of Ca_2Si films on single-crystal sapphire

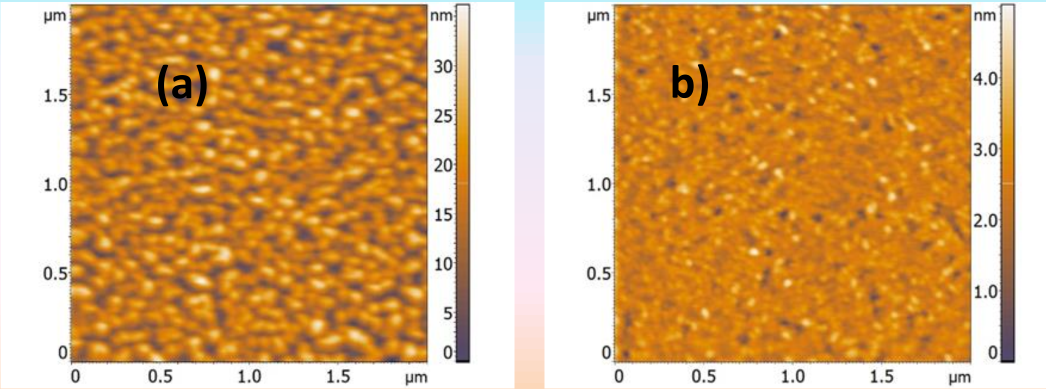

Figure 1. Morphology of **Ca_2Si films** grown on a sapphire substrate with (sample ***A***) and without (sample ***B***) using of **Mg_2Si/Ca_2Si template**. AFM scan images of sample ***A*** (**a**) and sample ***B*** (**b**).

The **morphology** of the grown films was studied by **AFM**. The film in sample ***A*** (Figure 1a) consists of densely intergrown round and oblong grains with sizes of **50 - 100 nm**. Their root-mean-square roughness is **4.44 nm**. The grains are randomly arranged on the substrate pointing out their weak crystallization on the surface. The film in sample ***B*** is almost atomically smooth with a root-mean-square roughness of **0.47 nm** (Figure 1b). It consists of grains with sizes of **20–50 nm** without noticeable faceting; therefore, it can be considered a ***nanocrystalline film***.

It has been established that in sample ***A*** on ***sapphire***, two peaks are observed from **$Ca_2Si(422)$**, related to the epitaxial relationship **$Ca_2Si(211)//Al_2O_3(0001)$** and from **CaSi(002)** (minor contribution) (***Fig. 2a***) .

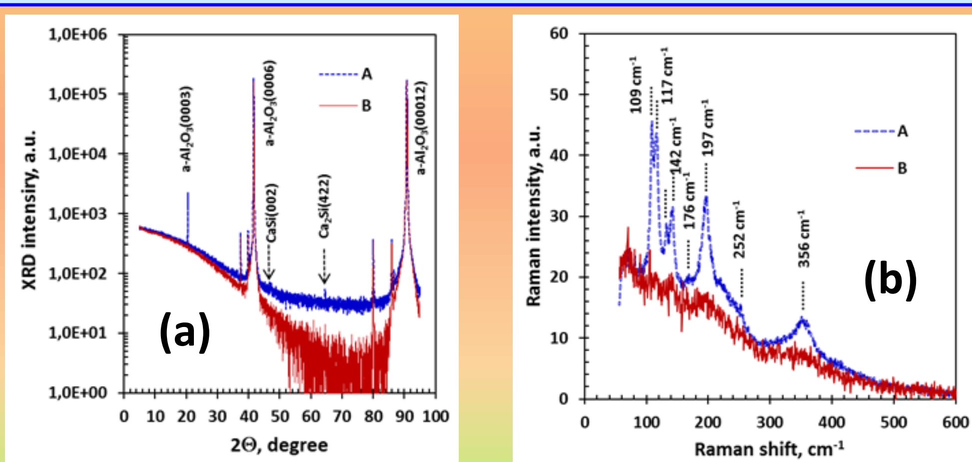

Figure 2. Structural characterization of **Ca_2Si films** grown on a sapphire substrate with (sample A) and without (sample B) using of **Mg_2Si/Ca_2Si template**. XRD patterns of (**a**) sample **A** and sample **B**. Raman spectra (**b**) for nanograin film in sample A and nanocrystalline film in sample B.

In sample ***A***, narrow and intense **Raman peaks** are observed at ***109, 117, 132, 142, and 197 cm^{-1}*** (***Fig. 2b***), which correspond well in intensity and position to the formation of Ca_2Si crystalline grains [8]. Sample ***B*** (Fig..2b) does not have pronounced peaks while the positions of the broadened peaks at ***120–200 cm^{-1}*** with low intensity (nanocrystalline state).

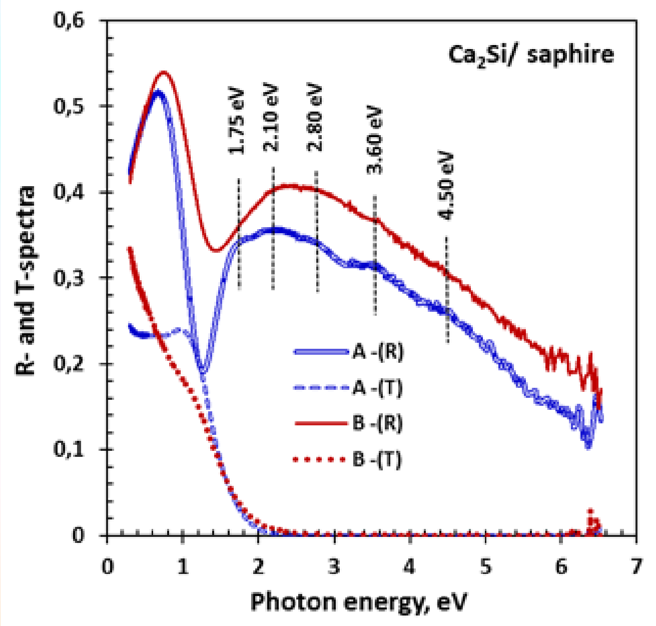

Figure 3. Spectra of transmission (T) and reflection (R) from the Ca_2Si /sapphire system for samples **A** and **B**.

The transmission (T) and reflection (R) spectra (Fig. 3) show the transparency of the Ca_2Si film in samples ***A*** and ***B*** to be up to photon energies of about 2.5 eV.

For a thicker film (***sample A***) there are peaks with energies of ***1.75, 2.1, 2.8, 3.6***, and ***4.5 eV***, which are close to the positions of the main peaks in epitaxial **Ca_2Si** films [8]. For the **Ca_2Si** film in sample **B**, these peaks are blurred because of its ***amorphous state***.

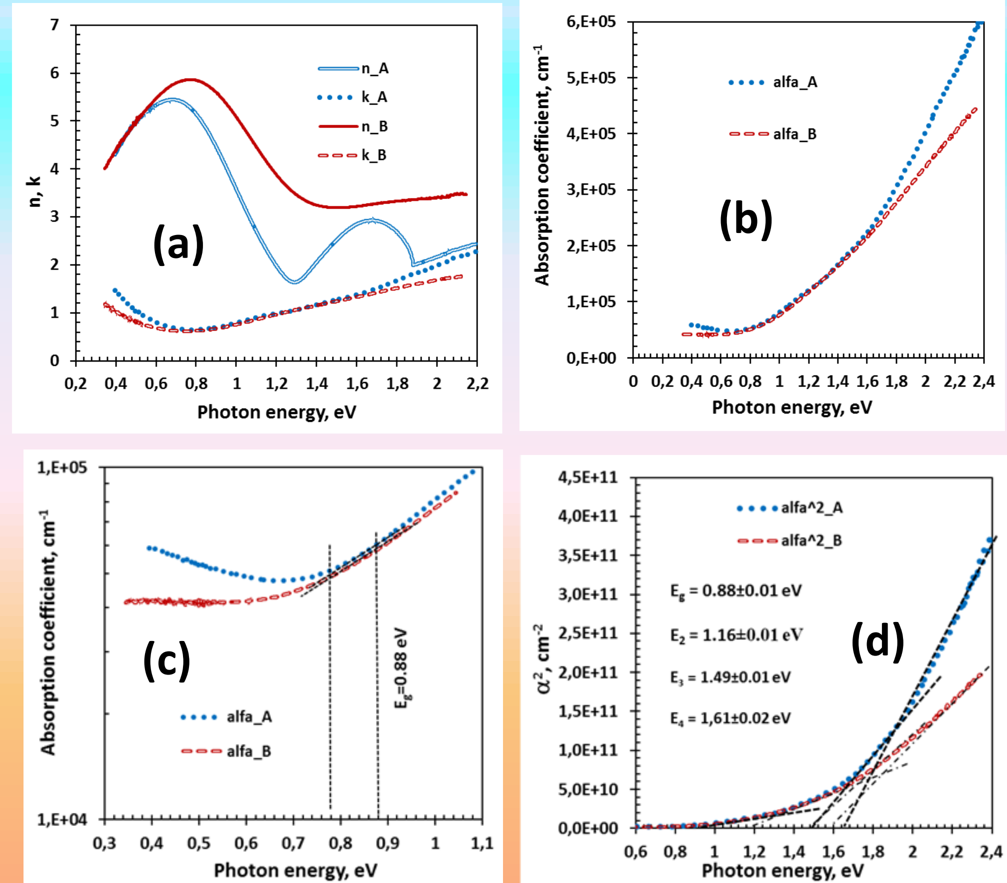

Figure 4. Spectra of (**a**) refractive index (***n***) and extinction coefficient (***k***), (b) spectra of absorption coefficient (α), (**c**) the dependence ***lgα*** from photon energy for determining the ***Urbach tail*** [9] and (d) absorption coefficient squared (α^2) for **Ca_2Si** films on a ***sapphire substrate*** in samples ***A*** and ***B***.

The fundamental direct interband transition was observed at energy **E_g=0.88±0.01 eV** both for nanocrystalline and amorphous **Ca_2Si films** on **sapphire**. The second direct interband transition has an energy **E_2=1.16±0.01 eV**, which is not very consistent with the one for the Ca_2Si epitaxial film on single-crystal silicon (E_2=1.095±0.15 eV) [8]. The *strongest third and fourth direct interband transitions* have energies **E_3=1.49±0.01 eV** and **E_4=1.61±0.02 eV**.

2.2 Morphology, structure and optical properties of Ca_2Si films grown on a Si(111) substrate with different Ca and Si flux ratios

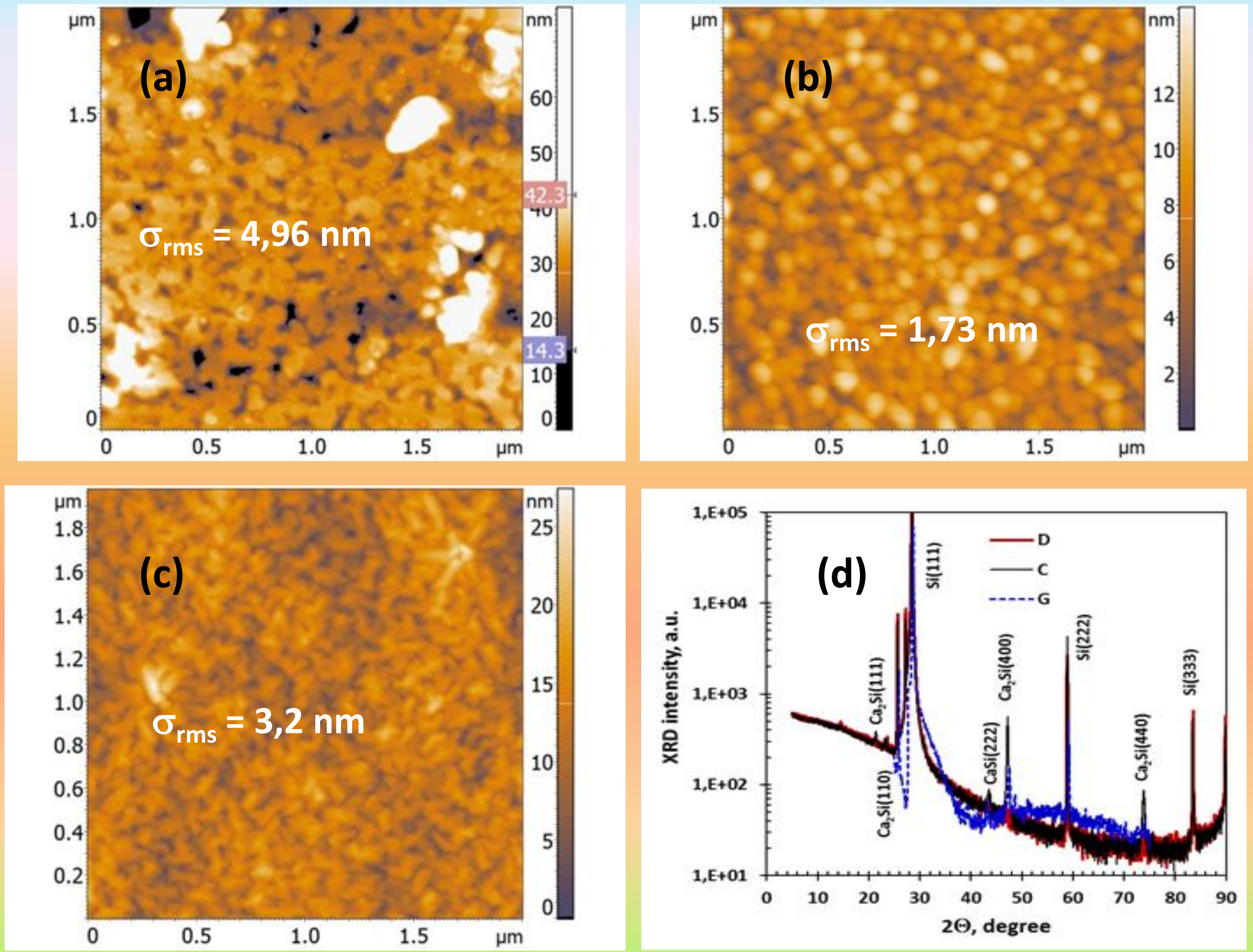

The film in sample ***C*** with a thickness of **30 nm** consists of intergrown grains with sizes of ***50-150 nm*** displaying some faceting (Fig.5a). In sample ***E***, a film with a thickness of about ***56 nm*** consists of non-oriented grains of a round and oblong shape (Fig. 5b) with sizes of ***50-100 nm***. The ***150 nm*** thick film (sample ***G***) consists of densely intergrown rectangular faceted nanocrystals of ***40x100 nm*** with some misorientation (Fig. 5 c).

In sample ***G***, only one **Ca_2Si phase** with the ***$Ca_2Si(100)/Si(111)$*** orientation is observed.

Figure 5. Morphology of **Ca_2Si** films grown on a *Si(111)* substrate for samples ***C*** (a), ***D*** (b) and ***G*** (c). XRD spectra for samples ***C, D*** and ***G*** with Ca_2Si films on Si(111) substrates (d).

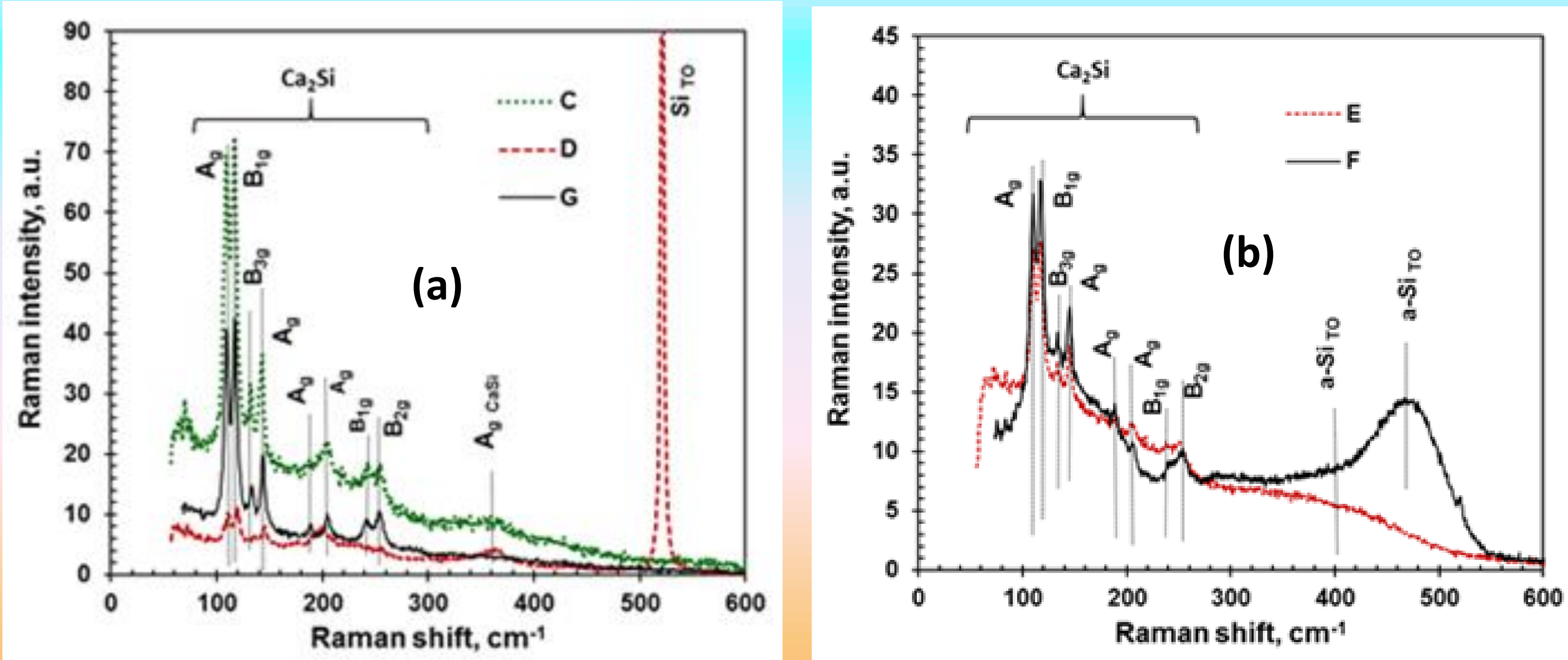

Figure 6. Raman spectra for five samples with Ca_2Si films on Si(111) for samples ***C***, ***D***, ***G*** without protective Si layer (a) and samples ***E*** and ***F*** with protective Si layer (b).

Identification of Raman peaks [**A_g** (***109.0; 143.0; 184.6 and 203.1 cm^{-1}***), **B_{1g}** (***116.5 and 238.4 cm^{-1}***), **B_{2g}** (***250.8 cm^{-1}***) and **B_{3g}** (***132.0 cm^{-1}***)] (Figure 6(a, b)) and their comparison with the previously published experimental data for epitaxial Ca_2Si films [8] confirmed the predominant contribution of the **Ca_2Si phase** to the structure of the grown films and their high crystalline quality. The appearance of a weak and broadened Raman peak at about ***360 cm^{-1}*** in samples ***C*** and ***D*** (Fig. 6a) indicates the presence of a small amount of the ***CaSi phase***, which has an intense peak at ***356 cm^{-1}*** even in the ***nanocrystalline state*** [10].

[9] J.I. Pankov. Optical Processes in Semiconductors, 2nd Revised ed. edition, Dover Books on Physics, New York, 2010; pp. 22-448.
[10] Galkin, N.G.; Galkin, K.N.; Tupkalo, A.V.; Fogarassy, Z.; Pécz, B., *J. Alloys and Compounds* **2020**, 813, 152101.

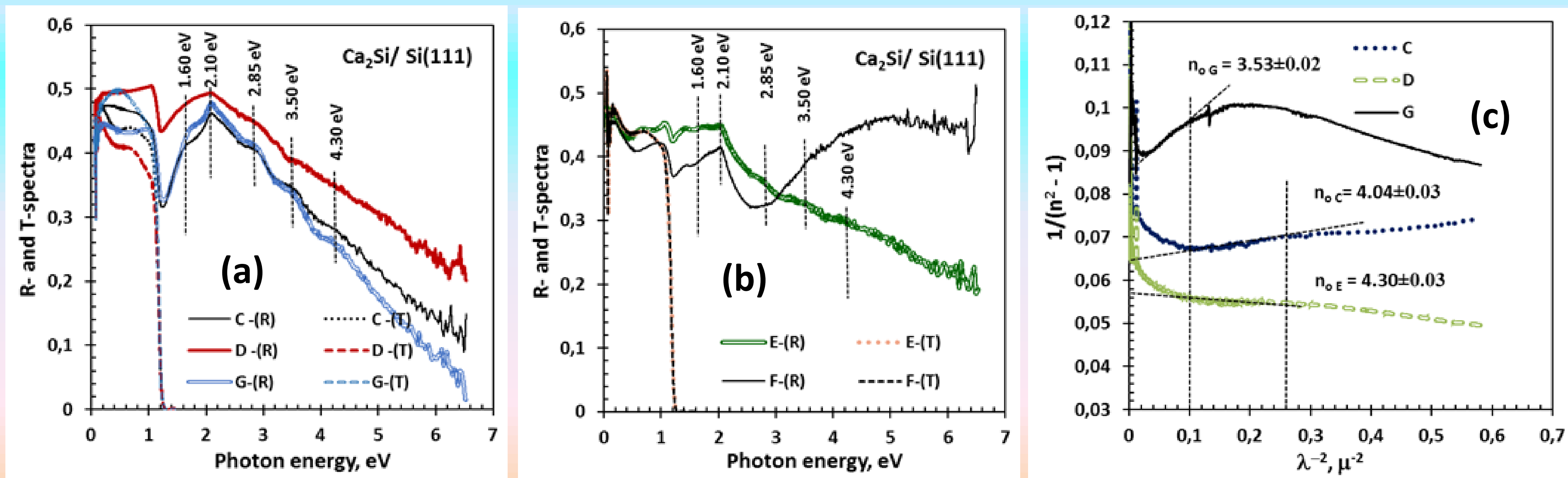

Figure 7. Spectra of transmission (T) and reflection (R for samples ***C***, ***D***, ***G*** (**a**) and samples ***E*** and ***F*** (**b**). Dependence of **$1/(n^2-1)$** on the λ^{-2} (**c**), where λ – is wavelength in micron (m). In (**c**), the vertical dotted lines show the boundaries of the transition to the dispersion-free region in samples ***C***, ***D***, and ***G***.

In general, the shape of the reflection spectra for grown ***Ca_2Si films*** (Fig. 7(a,b)) and the position of its peaks at energies from **1.3 eV** to 4.5 eV for Ca_2Si films not covered by silicon (Fig. 7a) are retained also taking into account **Ca_2Si** films on silicon [8] and **Ca_2Si** films on a ***sapphire substrate*** (Fig. 3). Additionally, a peak with energy of **1.6 eV** was resolved, which is related to **Ca_2Si**, but not to ***CaSi*** [10].

For films (samples ***C***, ***D*** and ***G***) dependences **$1/(n^2-1)$** on λ^{-2} (Fig. 7c) were plotted in order to determine the range of change in the dispersionless refractive index of films (n_o). These $\mathbf{n_o}$ values change from **3.53** for an epitaxial film with one ***$Ca_2Si(100)//Si(111)$*** epitaxial relationship (sample ***G***) to **4.04** and **4.30** (samples ***C*** and ***D***, respectively) for **Ca_2Si** films with three types of grains having epitaxial relationships ***$Ca_2Si(100)/Si(111)$***, ***$Ca_2Si(110)/Si(111)$*** and ***$Ca_2Si(111)//Si(111)$*** and a small contribution of grains of the ***semi-metallic phase CaSi***.

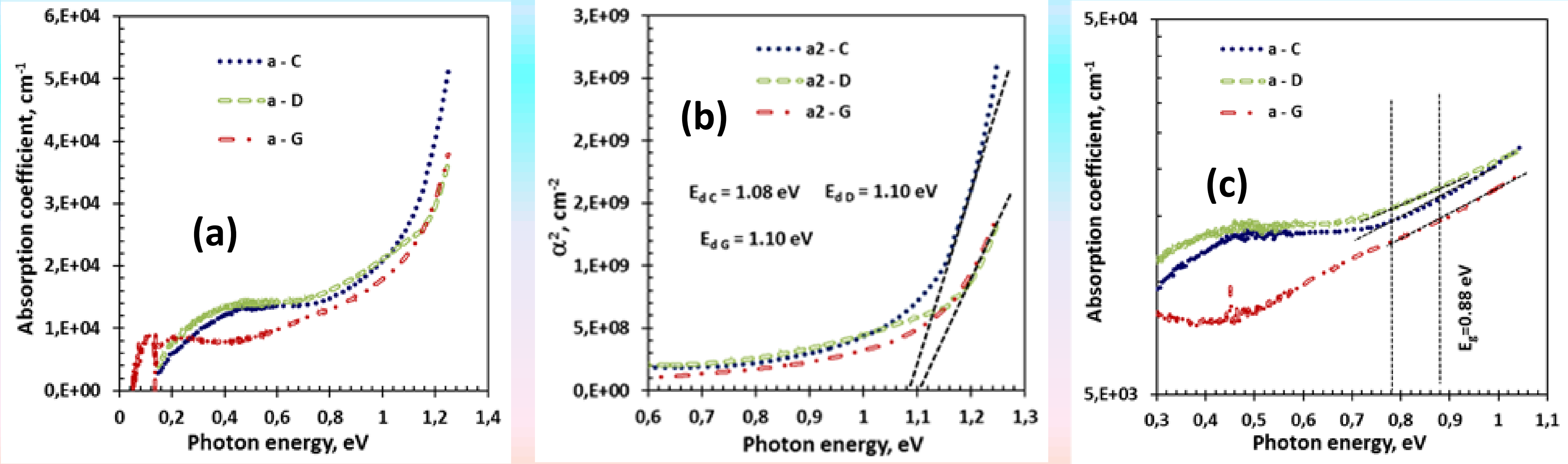

Figure 9. Optical absorption functions for **Ca_2Si** films on *Si(111)* on samples ***C, D*** and ***G.*** Spectra of the absorption coefficient (**a**), the square of the absorption coefficient versus the photon energy (**b**) and the dependence of **lgα** from photon energy for determining the Urbach tail [**9**] (**c**)

It can be seen that at photon energies of **0.4 - 0.8 eV** the values of ***α = (1.0 - 1.5) × 10^4 cm^{-1}*** of absorption coefficient are observed (Fig. 9a,b), which start increasing at photon energies above **0.8 eV** for all three samples due to absorption ***at interband transitions in Ca_2Si*** according to the data of theoretical first principle calculations [**11**].

At energies of ***0.7–0.9 eV***, the films should contain a fundamental transition, which is difficult to identify due to high absorption at the defect levels (***Urbach edge*** [**10**]), very low oscillator strength of the first direct transition [**12**]. The photon energy range from ***0.78 eV*** to ***0.88 eV*** is quite well described by the ***Urbach tail*** [**10**] (Fig. 9c), which was observed at the same energies in nanocrystalline and amorphous **Ca_2Si** films on ***sapphire*** (Fig. 4c).

[11] Lebegue, S.; Arnaud, B.; Alouani, M., Phys. Rev. B 2005, 72, 085103(1-8).
[12] Migas, D.B.; Miglio, L.; Shaposhnikov V.L.; Borisenko V.E., Physical Review B 2003, 67, 205203.

Conclusions

For the ***first time***, an original technique for growing oriented **Ca_2Si films** on single-crystal sapphire (**Al_2O_3(0001)**) using a sacrificial layer of two-dimensional magnesium silicide (**2D Mg_2Si**), which is easily transformed into **Ca_2Si** at **250 °C** in a **Ca** flow, has been developed and tested. For **Ca_2Si** films on ***Si(111)*** substrate, the effect of the ratio of the co-deposition rates of Ca and Si atoms at a temperature of **250°C** on the grain orientation was studied using a template technique by forming a sacrificial **2D Mg_2Si** layer. It has been established by XRD that at a ***high ratio of Ca to Si deposition rates*** (***7.3*** – ***20.0***), *oriented Ca_2Si films* are formed with three types of epitaxial relationships: ***Ca_2Si(100)/Si(111)***, ***Ca_2Si(110)/Si(111)*** and ***Ca_2Si(111)/Si(111)***, which provided ***compression*** of the ***Ca_2Si*** crystal lattice by **1.52%**. A **decrease** in the ratio of **Ca** to **Si** deposition rates to **4.0** made it possible to grow single-domain epitaxial films with the ***Ca_2Si(100)/Si(111)*** epitaxial relationship. A nanograin **Ca_2Si** film on **sapphire** has been grown displaying transparency up to **2.5 eV**. It has been established by optical spectroscopy and model calculations that the energy band structure of **Ca_2Si** contains ***four direct interband transitions***, including the ***fundamental one*** at **0.88 eV**. All the discovered facts can help in realizing the radiative transition and the ***photoelectric sensitivity*** of the ***Ca_2Si/Si*** diode structures in the near-IR region of the spectrum.